[34]E. Hutchisson, Phys. Rev. 36, 410 (1930).
[35]Reference 19, p. 106.
[36]A. R. P. Rau and U. Fano, Phys. Rev. A 4, 1751 (1971).
[37]Reference 19, p. 558.
[38]A. L. Farragher, F. M. Page, and R. C. Wheeler, Discussions Faraday Soc. 37, 205 (1964).
[39]J. A. D. Stockdale, R. N. Compton, G. S. Hurst, and P. W. Reinhardt, J. Chem. Phys. 50, 2176 (1969).
[40]K. Lacmann and D. R. Herschbach, Chem. Phys. Letters 6, 106 (1970).
[41]J. Berkowitz, W. A. Chupka, and D. Gutman, J. Chem. Phys. 55, 2733 (1971).
[42]Reference 19, pp. 457–459.
[43]G. Schulz (private communication).

PHYSICAL REVIEW A VOLUME 6, NUMBER 2 AUGUST 1972

Molecular Photodetachment Spectrometry. II. The Electron Affinity of O_2 and the Structure of O_2^-†

R. J. Celotta,* R. A. Bennett, J. L. Hall,‡ M. W. Siegel,§ and J. Levine‖
Joint Institute for Laboratory Astrophysics, Boulder, Colorado 80302
(Received 12 October 1971)

A beam of O_2^- ions, extracted from a glow discharge in N_2O, is crossed with the linearly polarized intracavity photon beam of an argon-ion laser (4880 Å). Electrons photodetached at right angles to the crossed beams are energy filtered by a hemispherical analyzer. The electron energy spectra are characteristic of photodetachment from the $v'=0$ state of O_2^- to the $X\,^3\Sigma_g^-$ and $a\,^1\Delta_g$ states of O_2. Vibrational state analysis is facilitated by the use of isotopes. The electron affinity obtained is 0.440 ± 0.008 eV. Additionally, we have measured the relative transition probabilities as a function of final vibrational state and the angular distributions of the outgoing electrons. The relative intensities, corrected by the angular distributions, determine through Franck-Condon-factor analysis the internuclear distance for the negative ion. We find $r_e'' = 1.341 \pm 0.010$ Å and therefore $B_e'' = 1.17 \pm 0.02$ cm^{-1}.

I. INTRODUCTION

Reactions involving molecular oxygen and its negative ion are of primary importance in understanding air chemistry, particularly in understanding D-region composition and processes. It is therefore not surprising that there is currently a great deal of interest in the electron affinity of molecular oxygen. There is a notably long history of O_2 electron-affinity determinations. Figure 1 shows all the determinations known to us plotted against their approximate publication date. Let us review briefly the techniques that produced these values.

The first determination of the O_2 electron affinity was made by Loeb.[1] Loeb determined the attachment energy by observing the energy required for detachment when an ion collides with a neutral molecule in a swarm-type experiment. His value of 0.34 eV is an upper limit. Bloch and Bradbury[2] used a model fitted to then current experimental data to arrive at an upper limit for the electron affinity of 0.17 eV. Massey[3] used rules for formulated by Mulliken,[4] to arrive at an electron affinity of about 1 eV. Since his argument assumed the electron affinity of O to be 2.2 eV, and we now know that it is 1.465 eV,[5] we can correct his predicted value to 0.27 eV. Pritchard[6] reviewing lattice energy calculations, concluded that 0.9 ± 0.1 eV was the most probable value for the electron affinity. Burch *et al.*[7] performed a photodetachment experiment and measured the cross section for photodetachment from O_2^- as a function of wavelength. Their measured cross section was found to be an excellent fit to the threshold form, derived by Geltman,[8] over an unexpectedly large region (0.4–2.5 eV). An extrapolation of the cross-section data to threshold provides a value of 0.15 eV for a detachment energy. By determining the appearance potential for the formation of O_2^- in a mass spectrometer, Curran[9] concluded that $E_A(O_2) \geq 0.58$ eV. Pack and Phelps[10] published a value of 0.46 eV obtained in a swarm-type experiment and later refined their value to 0.43 ± 0.02 eV. In these experiments the O_2^- ion had to survive approximately 10^8 collisions and was therefore expected to be in its lowest vibrational state. This value of the electron affinity (0.43 ± 0.02) eV has been the most widely accepted to date. Fischer *et al.*[11] studied charge transfer of H^- to O_2 and concluded that the electron affinity is greater than that of H (0.754 eV).[12] This experiment is contradicted by that of Dunkin *et al.*,[13] in which thermal charge transfer was not observed. Stockdale *et al.*[14] studied the dissociative attachment of electrons to NO_2 and from measured appearance potentials concluded that $E_A(O_2) \geq 1.1$ eV. However, depending on the calibration of the

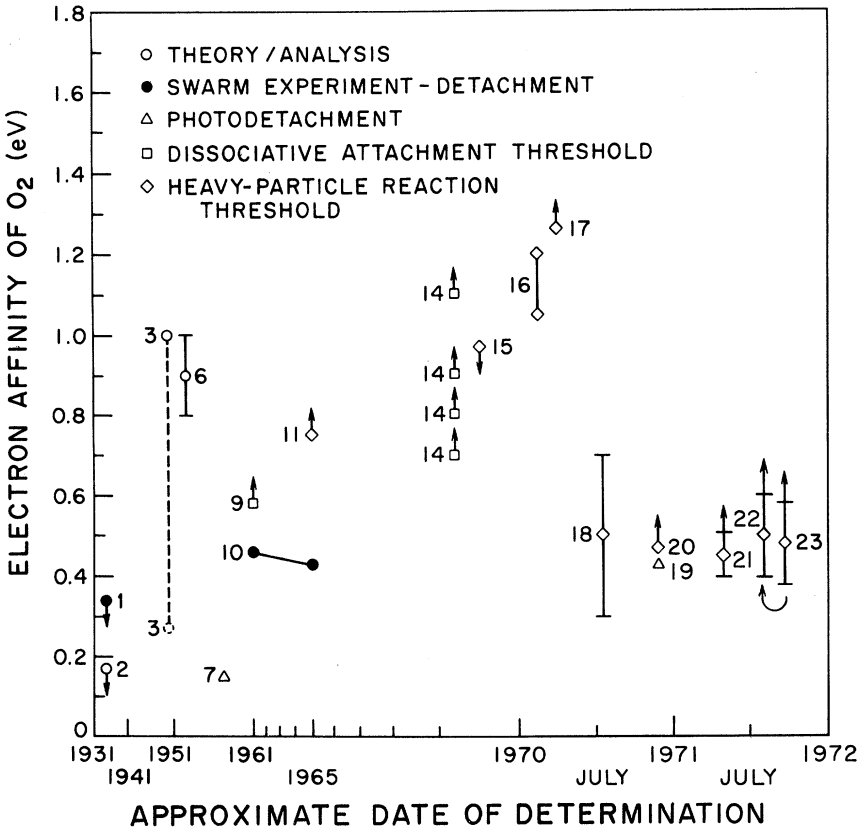

FIG. 1. Historical view of O_2 electron-affinity determinations. Arrows indicate the measurement was an upper or lower bound. The numbers refer to references.

energy scale used, values for lower limits of 0.9, 0.8, and 0.7 eV are possible. Fehsenfeld *et al.*[15] measured the electron detachment reaction

$$O_2(a\,^1\Delta_g) + O_2^- \rightarrow 2O_2 + e \qquad (1)$$

in a flowing afterglow apparatus and found it exothermic at thermal energies setting an upper limit for the electron affinity of 0.94 eV. Vogt *et al.*[16] studied charge-transfer reactions of H^-, SO^-, and ND_2^- on O_2. They concluded that the first two were exothermic and the last was endothermic. This allowed them to bracket the electron affinity of O_2 by 0.776 and 1.05 eV as lower bounds and 1.2 eV as an upper bound. Bailey and Mahadevan[17] concluded from a study of low-energy O^- collisions with O_2 that $E_A(O_2) \geq 1.265$ eV. Lacmann and Herschbach[18] measured cross sections for the ionization of K by low-energy O_2. Their measured threshold predicts an electron affinity of 0.5 ± 0.02 eV. Celotta *et al.*[19] reported a preliminary result of this determination as 0.43 ± 0.03 eV. Johnsen *et al.*[20] have investigated the O^- on O_2 charge-exchange reaction up to 3.0 eV in a drift tube. This procedure produced an electron affinity of about 0.47 eV or greater. Nalley and Compton[21] used $Cs + O_2$ scattering to arrive at a lower limit of 0.46 ± 0.05. Chantry[22] has obtained a lower limit of 0.50 ± 0.1 eV by careful analysis of the charge-transfer reaction of O^- on O_2. Finally, Berkowitz *et al.*[23] studied the threshold for the charge transfer from I^- to O_2. This enabled them to estimate a lower limit of 0.48 ± 0.1 eV for $E_A(O_2)$.

II. TECHNIQUE

The details of the technique utilized in this experiment as well as the complete theoretical justification are contained in the preceding paper[24] and only the most important points are mentioned here. The emphasis in the present paper is on the data and the conclusions that can be drawn.

A. Experimental Method

By illuminating a beam of negative ions with the intracavity beam of an argon-ion laser (4880 Å) we photodetach electrons from a fraction of the negative ions. Those electrons entering a small solid angle $4\pi/2000$ sr, at right angles to both the ion and photon beams are filtered by a hemispherical electron monochromator and, if transmitted, are detected by a particle counter and stored digitally. By sweeping the transmission energy, the energy spectrum of the photodetached electrons is accumulated. By conservation of energy, the vertical detachment energy E_{vd} for a characteristic

rotational temperature T, can be determined from the relation

$$E_{\mathrm{vd}}^{T}(v', v'') = h\nu - \Omega + E_{\mathrm{cp}} - (m/M)\,W\,, \qquad (2)$$

where v'' and v' are initial and final vibrational states, respectively, $h\nu$ is the incident photon energy (2.540 eV), Ω is the outgoing electron's measured lab-frame energy, m/M is the ratio of the mass of the electron to the mass of the ion, W is the kinetic energy of the ion, and E_{cp} is a contact potential term. The last term in Eq. (2) comes from the coordinate transformation to the laboratory system. This equation holds for mutually perpendicular photon, ion, and electron beams. Terms having to do with mechanical misalignments and higher-order terms yielding very small kinetmatic effects have been tested for and shown to be negligible.[24] Once an energy spectrum is taken, the problem is reduced to identifying the initial and final states corresponding to each of the measured vertical detachment energies. A detailed discussion of the techniques utilized is presented in the preceding paper; the most salient arguments will be repeated in Sec. IV. It is sufficient to say here that the expected electron energy spectrum will be characterized by a series of peaks, each one corresponding to transitions between different initial-final vibrational state pairs. Each peak will have a width originating in the fine-structure splittings of the negative-ion state, the finite resolution of the electron transmission filter, and the distribution in energy of the various molecular rotational levels present. The contact potential term E_{cp} can be eliminated by using the mass programmer to alternate the beam between O^- and O_2^- every 8.3 msec (a time short compared to contact potential variations), and to store the two ions' photodetachment spectra separately. Since the electron affinity of O is very accurately known,[5] the contact potential term can be eliminated and the energy scale is then absolute.

We also measure the angular distributions of the emitted photoelectrons. The argon-ion laser light is linearly polarized, and with the aid of a rotatable half-wave plate within the laser cavity, the plane of polarization is rotated. By accumulating the photodetachment signal at a fixed energy, i.e., for a particular transition $O_2(v', v'')O_2^-$, as a function of the angle between the outgoing electron's momentum and the electric field vector of the light, the angular distribution can be measured. To do this the photodetachment signal and the product of the laser intensity and the ion-beam current are simultaneously digitally stored as a function of half-wave-plate angle. This allows us to normalize the data and removes the effect of beam drifts and laser intensity fluctuations.

B. Source Conditions

The source used was a hot cathode-type glow discharge with off-axis extraction. When 55 μ of N_2O was used as the source gas and a 0.03-cm-diam tungsten filament was used as the cathode, beams of 10–20 nA of O_2^- were produced in the interaction region. Other gases (O_2, O_2+He, CO_2) as well as other sources (duoplasmatron and hollow cathode glow discharge) were studied in unsuccessful attempts to generate useful O_2^- beams. Where a suitable beam current was obtained the O_2^- appeared to be excessively vibrationally excited. The present source could be operated for long periods of time using thoria-coated iridium filaments, but the use of these filaments reduced the beam current by a factor of 2. A partial pressure of 2–8 μ of O_2 added to the 55 μ of N_2O increased the O_2^- beam current by approximately 30%. A full description of the source, including a mass spectrum obtained with N_2O as the source gas, is presented in the preceding paper.[24]

III. DATA

A. Overview

The photodetachment data shown in Fig. 2 give an over-all view of the spectrum observed. Although the signal-to-noise ratio shown is not optimum, this set of data illustrates all of the features to be discussed later in detail. The number of ejected photoelectrons collected is shown as a function of the transmission voltage of our electron energy filter system. Apart from various corrections, the x axis is therefore the energy difference between the incident photon energy and energy required for the transition from an initial state $O_2^-(v'')$ to a final state $O_2(v')$. The data exhibit nine prominent peaks and there appears to be a double-humped intensity envelope of the peak heights. It should be noted that the fourth and ninth peaks from the left are anomalously wide and there appears to be a very small peak just to the right of the ninth peak. Each peak is labeled by its transition assignment as derived below.

B. Detailed Data on Peak Pairs

In order to study the energy difference between adjacent transition peaks as well as to measure the relative intensity of neighboring transitions, data were accumulated as illustrated in Fig. 3. Here again the number of detached photoelectrons is plotted as a function of energy. Also plotted is a least-squares fit[24,25] of the data by a function which is the sum of two slightly asymmetric Gaussians. These peaks correspond to the $X O_2^-$

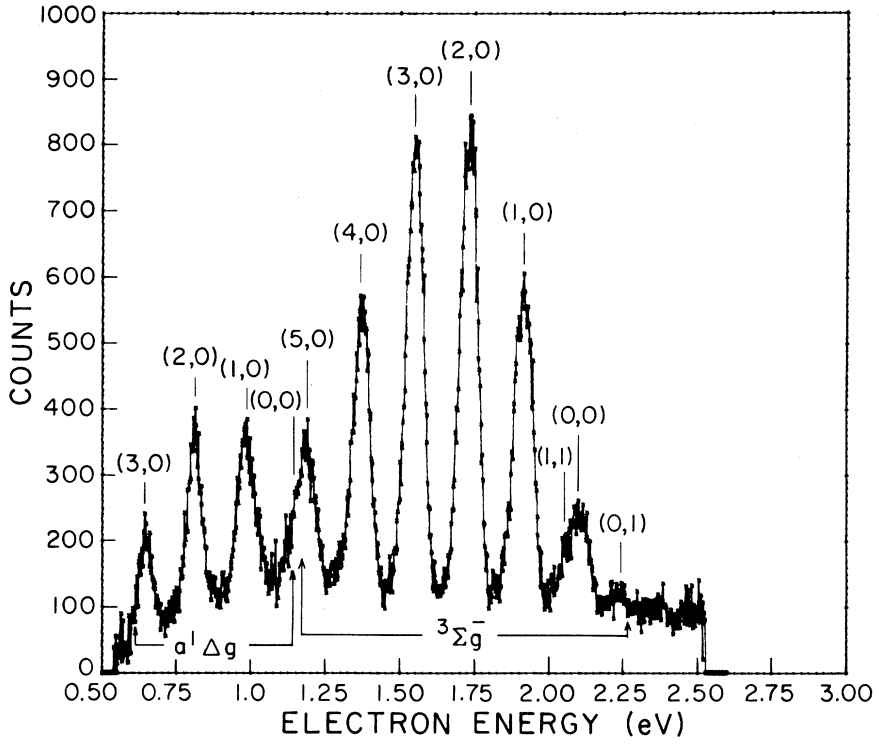

FIG. 2. Over-all view of the O_2^- photodetachment spectrum.

$(3, 0)O_2^-$ and $X O_2(2, 0)O_2^-$ transitions.

C. Angular-Distribution Data

An angular-distribution measurement was performed for each of the resolvable transitions shown in Fig. 2. The transmission energy of the electron filter was set at the center of the peak in the energy spectrum corresponding to the transition of interest and the polarization direction of the laser light was varied relative to the electron collection direction. Figure 4 shows the resulting angular distribution, and the theoretical[26] curve least-squares fitted[25] to the data. The x axis is the polarization angle, which goes through 4π as the half-wave plate physically moves through 2π. The data shown on this figure have been corrected for background counts and beam and laser power fluctuations.

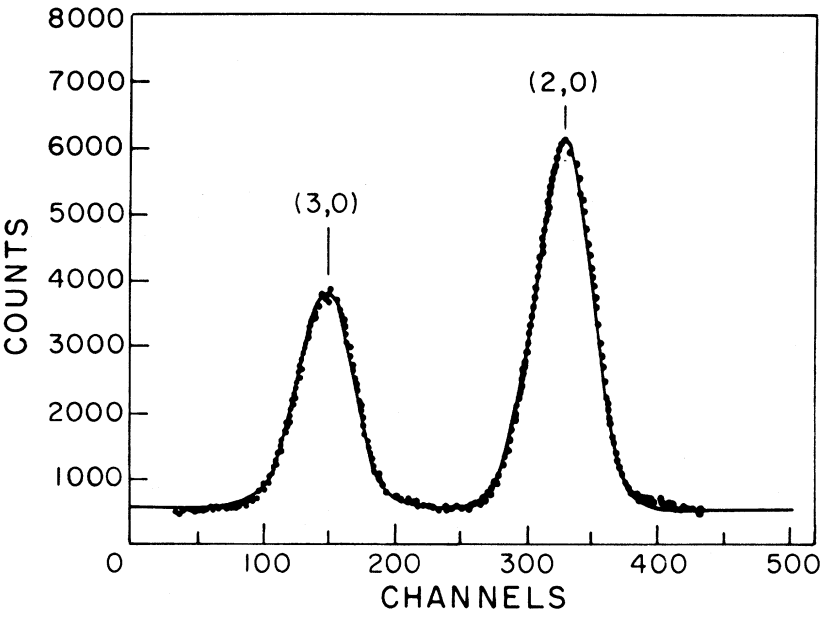

FIG. 3. Detailed look at the O_2^- $(3, 0)O_2^-$ and $O_2(2, 0)O_2^-$ transitions. Each channel represents an energy interval of 4.89 meV.

IV. RESULTS

A. Transition Identification

As in all molecular photodetachment experiments, care must be exercised in the determination of the initial and final vibrational states corresponding to the observed transitions. A significant difference in the equilibrium internuclear separations of the neutral and the negative ion could cause the Franck-Condon principle to operate so as to make the $X\,O_2(0,0)O_2^-$ transitions have less than the minimum observable strength. It is therefore possible that the electrons observed to possess the highest energy correspond to the $X\,O_2(v',0)O_2^-$ transition where v' is not zero. It is also possible that the ions are produced in the source in predominantly one vibrational state, which is not the ground state. Although this conjecture is a bit extreme, at a minimum one might expect some transitions from vibrationally excited states.

We shall demonstrate that the transition labeling as shown in Fig. 2 is correct; i.e., we will prove that the observed transitions are from O_2^- which is predominantly in the $X^2\Pi_g(v''=0)$ state, to the series of final states which are the ground-state O_2 vibrational states, $X^3\Sigma_g^-(v'=0,1,2,3,4,5)$, and the vibrational states of the first electronically excited state of O_2, $a^1\Delta_g(v'=0,1,2,3)$.

Examination of the data shown in Fig. 2 reveals a series of peaks, each spaced by approximately the vibrational interval of the neutral O_2 $X^3\Sigma_g^-$ ground state. It can be concluded that we are seeing transitions from a single initial vibrational state to a series of final states instead of from a series of initial states to one final state. There are two major reasons why this contention is true. First, the peak spacings are characteristic of the O_2 neutral vibrational intervals which are about 45% larger than the known[27,28] O_2^- intervals. Second, when the peak spacings are measured more accurately they reveal an anharmonicity such that the peaks become more closely spaced with decreasing outgoing electron energy. This situation would arise in the one initial-state model but the converse would be true if we were seeing transitions from many initial states to one final state.

The 4880-Å radiation used makes the $a^1\Delta_g$ state of the O_2 neutral energetically accessible. In this regard it should be noted that the intervals between the left-most peaks in Fig. 2 were characteristic of the $a^1\Delta_g$ states while those on the right were associated with the $X^3\Sigma_g^-$ state of O_2. The fourth peak from the left can be seen to be significantly wider than the others. A more detailed experiment shows it to be 30% wider than the other peaks (with the exception of right-most peak, which will be discussed later). This fourth peak from the left is formed from the overlap of two peaks, one from the $a^1\Delta_g$ vibrational series and one from the $X^3\Sigma_g^-$ vibrational series. It is clear that we are seeing the sum of two series of final states rather than merely one series because the measured energy intervals are characteristic of the $X^3\Sigma_g^-$ on the right and $a^1\Delta_g$ on the left and also because the obvious overlap between the two series produces the anomalously wide peak. There is no question about the identification of the two series although at this point we cannot yet say what is the lowest observed vibrational state of each of these progressions.

To determine the vibrational quantum number for the single initial state of the ion we can use some general rules resulting from the Franck-Condon principle. The intensity of the transitions from the $X^2\Pi_g(v''=0)$ state to the progression $X^3\Sigma_g^-(v'=n,n+1,\ldots,n+5)$ can be represented by a single-humped function of v'. The transition probability rises from a small value for $v'=1$, reaches a maximum, and then falls to zero for large v', in a smooth way. This behavior is also characteristic of the progression in the $a^1\Delta_g$ final state. As a general rule, only the Franck-Condon factors connecting the $v''=0$ state to the progression of upper vibrational levels exhibit this behavior.[29] Intensity envelopes for transition strengths, in absorption, will, in general, exhibit at least one minimum if the lower state

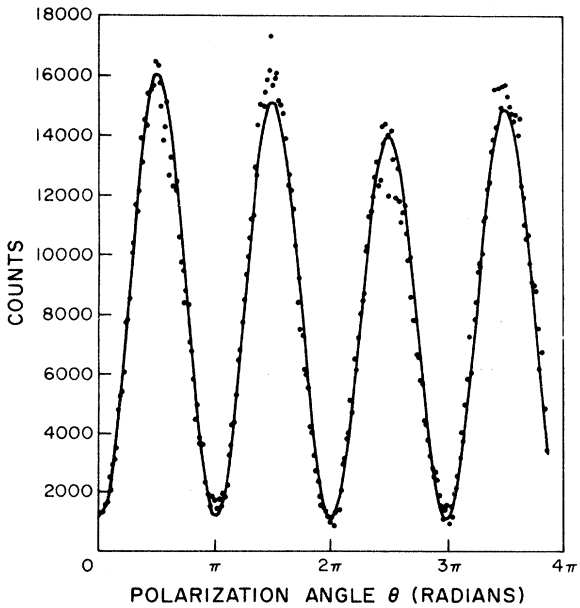

FIG. 4. Plot of the count rate as a function of the polarization angle θ. The dots are experimental points and the smooth curve is the least-squares fit to the theoretical form. Data are for $O_2(3,0)O_2^-$ transition.

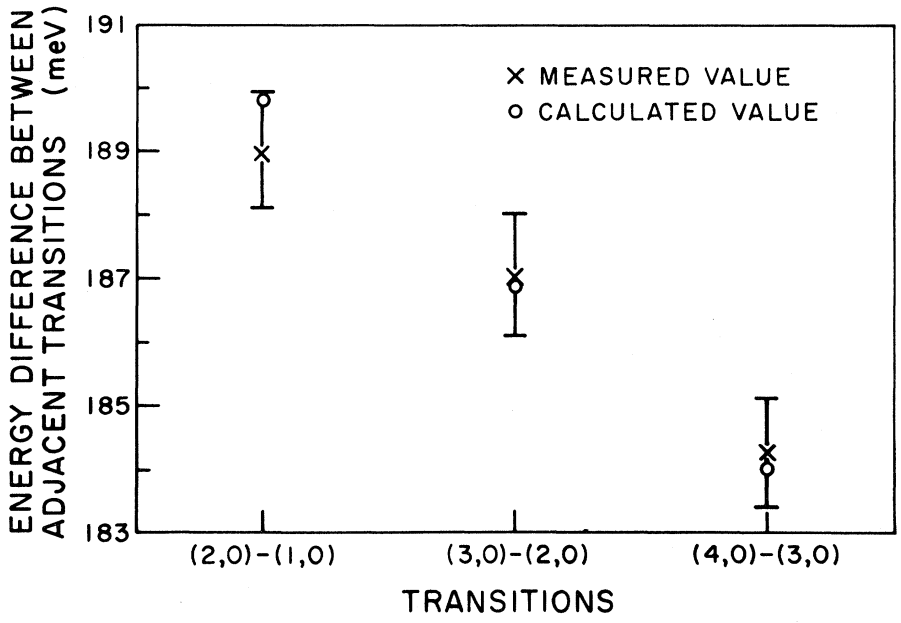

FIG. 5. Comparison between the measured and calculated energy difference between adjacent transition peaks.

is other than $v'' = 0$. Since the measured intensity envelope has a single-humped shape in both transition series we can conclude that the single vibrational state of the negative ion is, as expected, $v'' = 0$. As a check, Franck-Condon-factor intensity envelopes were calculated[24] between various vibrational levels of a negative-ion Morse potential and the series of upper-state vibrational levels. For any reasonable values of the Morse-potential parameters the $v'' = 0$ progression produced the required single-humped envelope and no other progression could be misinterpreted in such a way as to give the required shape.

To establish the final vibrational state numbering three techniques are used.[24] Each method is independent of the other two and is sufficient to determine the identification. The first, and most obvious, is to measure the spacing between the peaks with great accuracy, as is shown in Fig. 3. These spacings are derivable from the spectroscopically known O_2 vibrational energy levels,[30] and, since the potential is anharmonic, an unambiguous state identification will result. Measurements were made of the energy differences between the four largest peaks. These peaks were chosen, not only because they can provide the largest signal-to-noise ratio, but also because there is little structure near their bases to interfere with the fits of the data. The $a\,^1\Delta_g$ series was not used because far less is known about its potential.[31] The results of this experiment are shown in Fig. 5. The error bars on the measured splittings are primarily due to the calibration of the energy scale used in measurement. The transition identification given in Fig. 2 results from this determination.

Because of the high accuracy required of the energy-interval determination we found it necessary to calibrate the energy scale of our monochromator.[24] The energy-scale calibration is obtained in two ways: One technique measures the electron affinities of O and S simultaneously. Since this is explained in detail in the preceding paper, we will not dwell on the point. The final result of this calibration is that all measured energy differences should be multiplied by 1.03 ± 0.005. As an alternate measurement of the calibration factor we measured the separation between the (1, 0) peak of $X^3\Sigma_g^-$ series and the (1, 0) peak of $a\,^1\Delta_g$ series. Since $\Delta G_{1/2}$ is very accurately known for both states,[31] and the term energy is precisely known,[31] this measurement provides an even more exacting test of the energy scale. The result of this determination is an energy correction factor of 1.031.

A second technique that can be used to provide a state identification is Franck-Condon-factor analysis. As will be explained below, one can determine a Morse potential for the negative ion by varying the Morse-potential parameters until the observed transition strengths agree, in a least-squares sense, with the predictions of the Franck-Condon factors. In the present case the values of ω_e'' and $\omega_e x_e''$ are known from other work,[27,28] so these parameters were not left free to vary. As a result, when the r_e'' of the O_2^- Morse potential is varied a best fit is obtained at one value. If the vibrational state assignment for the final state is changed and another best fit is calculated it is found that the optimum fit occurs for the state assignment given in Fig. 2. For a misidentification of the upper-state level, the sum of the squares of

the residuals of the fit increase by an order of magnitude.

The third technique utilized in determining the vibrational state assignments for the O_2 final state is isotope substitution. Neglecting rotational effects and cubic and higher terms, the energy for a particular transition is[24]

$$\nu = \nu_e + \omega_e'(v' + \tfrac{1}{2}) - \omega_e x_e'(v + \tfrac{1}{2})^2 - [\omega_e''(\tfrac{1}{2}) - \omega_e x_e''(\tfrac{1}{2})^2] . \quad (3)$$

In Eq. (3) we have put $v'' = 0$ and ν_e is the electronic-term energy. If Eq. (3) is rewritten for an isotope of O_2, we get

$$\nu^i = \nu_e + \rho\omega_e'(v' + \tfrac{1}{2}) - \rho^2\omega_e x_e'(v' + \tfrac{1}{2})^2 - [\rho\omega_e''(\tfrac{1}{2}) - \rho^2\omega_e x_e''(\tfrac{1}{2})^2] , \quad (4)$$

where ρ^2 is the ratio of the reduced masses of the molecules

$$\rho^2 = \mu/\mu_i . \quad (5)$$

Subtracting Eq. (4) from Eq. (3), we get

$$\nu - \nu^i = (1-\rho)\omega_e'(v' + \tfrac{1}{2}) - (1-\rho^2)\omega_e x_e'(v' + \tfrac{1}{2})^2 - [(1-\rho)(\tfrac{1}{2}\omega_e'') - (1-\rho^2)(\tfrac{1}{4}\omega_e x_e'')] . \quad (6)$$

Equation (6) gives the isotopic shift in energy of a transition in terms of known quantities and v', the required final vibrational state identification. The experiment performed consists of measuring the outgoing electron energy corresponding to the same transition for $^{16}O_2^-$ and $^{18}O_2^-$. We electronically switch the mass filter between isotopes every 8.3 msec and record the photodetachment peak corresponding to, for example, the $O_2(2, 0)O_2^-$ transition for both isotopes. The energy difference between peak centers is carefully determined using least-squares curve-fitting techniques[25] and Eq. (6) is used to calculate the final-state vibrational quantum number. For the transition labeled $O_2(3, 0)O_2^-$ we find $v' = 3.14 \pm 0.18$ and for the transition labeled $O_2(2, 0)O_2^-$ we find $v' = 1.85 \pm 0.18$. Hence the isotope experiments provide the same identification of the final vibrational states as do the two other techniques.

Figure 2 shows that the peak corresponding to the $O_2(0, 0)O_2^-$ transition is anomalously wide. Also, there is a rather small peak to the right of the (0, 0) peak labeled (0, 1). This peak can be identified as corresponding to a transition from the relatively sparsely populated $v'' = 1$ state of O_2^- to the $v' = 0$ state of XO_2. It may be observed that the weak peak is approximately 0.135 eV more energetic than the (0, 0) transition. The value 0.135 eV is approximately ω_e for O_2^-.[27,28] The (0, 0) transition peak is then broadened by the overlap of the (1, 1) transition, which produces an outgoing electron of 0.196 eV less energy then the (0, 1) transition where 0.196 eV is the vibrational interval in O_2. It is possible to find some operating conditions such that the population of these initial excited vibrational states is either greater or less than shown. With increased excited-state populations we can get a direct check on the value of ω_e for O_2^- which is in agreement with the previously mentioned values.[27,28] Usually the source is run so as to minimize the excited vibrational populations so that they will not interfere with precision measurements of the energy difference between peak centers or peak area determinations.

B. Relative Transition Strengths

In order to calculate the relative strengths of the $XO_2(1, 0)O_2^-$, (2, 0), (3, 0), and (4, 0) transitions two types of measurements were needed. Neighboring transitions were observed pairwise, as shown in Fig. 3, with the polarization of the light set for a maximum counting rate. The least-squares fit[25] of these data is then integrated over each line and checked by a direct numerical integration of the data. By themselves, these integral line strengths would provide a rough indication of the relative transition intensities: They must be corrected for the angular distribution of ejected electrons which varies as a function of outgoing electron energy, i.e., from transition to transition.

The angular distributions were measured for all of the resolvable peaks shown in Fig. 2. The theoretically expected angular distribution[26] is

$$I(\theta) = A[1 + \beta P_2(\cos\theta)] . \quad (7)$$

In Eq. (7), θ is the angle between the electric field vector of the light and the electron-collection direction as measured in the plane perpendicular to the photon beam, [24] P_2 is the Legendre polynomial, and β is the anisotropy parameter which may range in value from $+2$ to -1. For $\beta = +2$, Eq. (7) becomes $I(\theta) \propto \cos^2\theta$ and for $\beta = -1$ it becomes $I(\theta) \propto \sin^2\theta$. For the $^2\Pi_g$ state of O_2^- electric dipole transitions will produce outgoing p and f electrons which interfere to produce the angular distribution. In the energy range we discuss, the outgoing electrons will be predominantly p wave.

To compensate for a small variation in the spatial overlap of the ion and laser beams as a function of half-wave-plate angle, an additional multiplicative term $\sin(\frac{1}{2}\theta + \delta)$ was inserted in the fitting function.[24] Since the polarization direction rotates through 4π when the half-wave-plate rotates through 2π, any overlap effect will recur at half the polarization frequency and will not affect the value of β given by the fit. The function fitted to the data, as shown in Fig. 4, is

$$I(\theta) = A[1 + C\sin(\tfrac{1}{2}\theta + \delta)][1 + \beta P_2(\cos\theta)] . \quad (8)$$

The variation of β as a function of the outgoing elec-

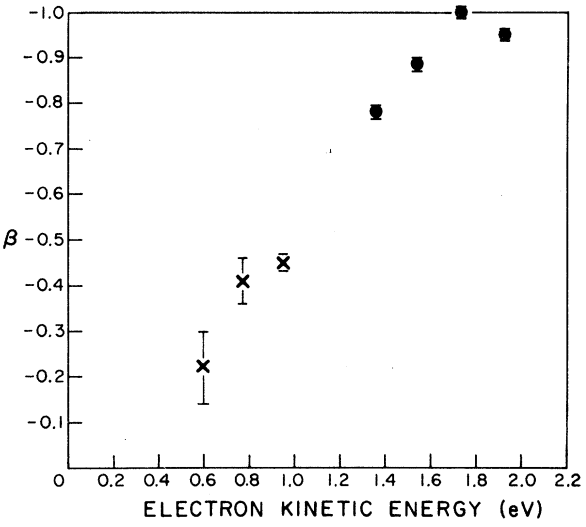

FIG. 6. Plot of the anisotropy parameter β as a function of the outgoing electron's kinetic energy. ●: events in which the final state is $X\,^3\Sigma_g^-$. ×: events in which the final state is $a\,^1\Delta_g$.

trons energy is shown in Fig. 6. As expected, β has a value near zero (s wave) close to threshold, approaches -1 with increased electron energy, and finally turns down again toward $+2$.

In Table I, the results of the angular-distribution measurements and the relative intensity measurements are summarized. The error estimates are standard deviations and are arrived at by the fitting program from an analysis of the error in each data point and its effect upon the determination of the value of β. The area determinations are accurate to approximately $\pm 2\%$.

C. Determination of r_e''

In order to use the measured relative intensities of transitions to determine a Morse potential for the negative-ion state a few assumptions must be made. To use the Franck-Condon principle we assume the Born-Oppenheimer approximation to be valid and the Franck-Condon principle in turn assumes that the electronic transition moment does not change much over the first few vibrational levels of the ground-state neutral O_2. We look in a photon energy range far above the threshold region and use the vibrational overlap integrals alone as the predictor of relative transition strengths.

Overlaps are calculated, using the programs RKR, MORSE, and FCF,[32] between the numerical eigenfunctions of the very precise RKR potential for O_2 and those of a parametrized Morse potential for O_2^-. The resulting ratios of predicted transition probabilities are compared to the ratios obtained experimentally, and the Morse-potential parameters are varied to obtain their most probable values in a least-squares sense. The residuals of the least-squares fit are very sensitive to the value of r_e'' chosen for the negative-ion Morse potential. The sum of the squares will typically double if the value of r_e'' is offset 0.001 Å from its optimum position. The sum of the squares of the residuals is not as sensitive to the value of ω_e'' as it is to r_e''. A change in ω_e'' of 80 cm^{-1} is required to change the sum of the squares by a factor of 2. These numbers demonstrate the sensitivity of the procedure and not its accuracy. In order to know the accuracy we must know both what error is made in measuring the relative transition strengths and how well the Franck-Condon factor should be able to account for these relative strengths. An error in the measured relative intensity data would occur if the transmission of our electron energy varied as a function of transmission energy. While care has been taken to avoid such difficulties and we have evidence[24] that no large error is present, it is difficult to demonstrate that no variation exists. We are using the electron energy interval of 1.4–2.0 eV to observe the $X\,O_2(1, 0)O_2^-$ through $X\,O_2(4, 0)O_2^-$ transitions, and this does not present a large dynamic range to the analyzer or the electron optics.

It is difficult to find a good guide to the errors induced by the theoretical assumption that the electronic matrix element is a slowly varying function of energy which can be assumed constant over our limited energy range. To overcome this problem we drastically overestimate the possible size of the

TABLE I. Summary of angular distribution and relative intensity measurements.

Transitions	Peak area	β	Corrected area	Intensity ratio
(3,0)	67 518 ± 1350	−0.8880 ± 0.0053	46 758 ± 9350	1.673 ± 0.050
(4,0)	38 941 ± 7780	−0.7865 ± 0.0066	27 949 ± 5600	
(2,0)	40 353 ± 8071	−1.0000 ± 0.0100	26 902 ± 5400	1.100 ± 0.033
(3,0)	35 303 ± 7060	−0.8880 ± 0.0053	24 448 ± 4890	
(1,0)	23 446 ± 4690	−0.9492 ± 0.0050	15 900 ± 3180	0.6409 ± 0.019
(2,0)	37 212 ± 7445	−1.0000 ± 0.0100	24 808 ± 4690	

effect in our error calculations. In order to arrive at an error estimate on the value obtained for r''_e, we shall make the quite conservative assumption that the sum of the errors introduced by the transmission function of the analyzer and the theoretical assumptions is less than if the measured relative intensities were systematically wrong by a factor of 50% over the 0.6-eV range. The measured relative intensities were therefore "corrected" by a hypothetical transmission function which varied by ±25% over the 0.6 eV range and the change in the optimum r''_e was used as an estimate of the error in r''_e. Since ω''_e, and $\omega_e x''_e$ are available from other data[27,28] we shall keep these parameters fixed in our fits and determine only a value of r''_e.

The fitting procedure, using the programs mentioned above and the parameters $\omega''_e = 1089$ cm^{-1}, $\omega_e x_e = 12.1$ cm^{-1}, and $J = 13$, gave a best fit for r''_e of 1.341 Å. The error estimate for r''_e is ±0.010 Å. Using the equation

$$B''_e = B'_e(r'_e/r''_e)^2$$

we obtain a value of $B''_e = 1.17 \pm 0.02$ cm^{-1}.

D. Determination of Electron Affinity

To arrive at a value for the electron affinity of O_2, the energy of the observed $X\,O_2(0, 0)O_2^-$ transition must be determined, and then this value must be corrected for the electronic splitting of the negative ion $X\,^2\Pi$ state and rotational effects. The contact potential term in Eq. (2) is eliminated by using a calibration ion O^- in which case Eq. (2) is rewritten

$$E^T_{vd}(0, 0) = E_A(O) + \Omega(O) - \Omega(O_2; 0, 0) + m\,W\left(\frac{1}{M(O)} - \frac{1}{M(O_2)}\right), \quad (9)$$

where $E_A(O)$ is the electron affinity of O, the Ω's are the measured outgoing electron energies, the $\Omega(O)$ from O^- and the $\Omega(O_2; 0, 0)$ corresponding to the $X\,O_2(0, 0)O_2^-$ peak, and $M(O)$ and $M(O_2)$ are the masses of O and O_2, respectively. Because of the overlap of the $X\,O_2(0, 0)O_2^-$ peak with other structure, a measurement of the difference in energy between $X\,O_2(0, 0)O_2^-$ peak and the peak corresponding to O^- photodetachment is not practical. This is not important, however, because the O_2^- transitions differ in energy by the well-known spectroscopic energy levels of the neutral molecule. For this reason we measured the vertical detachment energy corresponding to the $X\,O_2(v' = 2) \leftarrow O_2^-(v'' = 0)$ transition $E^T_{vd}(2, 0)$ by measuring the energy difference $\Omega(O) - \Omega(O_2; 2, 0)$. Two measurements were made of this energy difference and the values obtained were 655.5 ± 0.8 and 654.9 ± 0.9 meV, which average to 655.2 ± 0.6 meV. The errors indicated

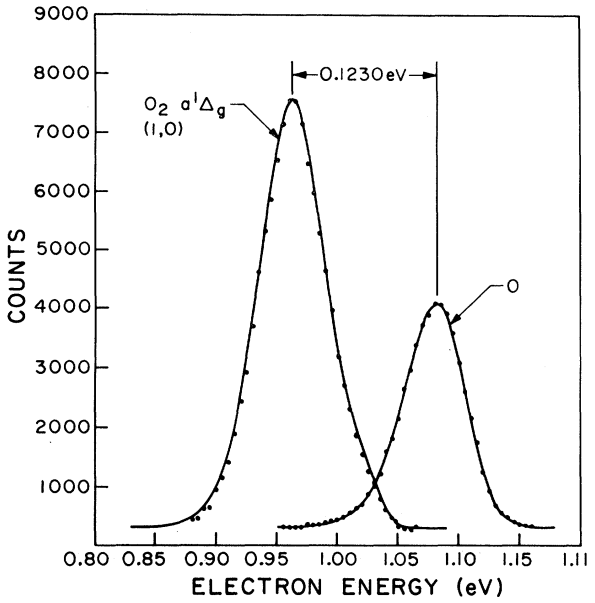

FIG. 7. Experimental data (dots) and the least-squares fit used in the electron-affinity determination. The curve on the left contains a small contribution from the $X\,O_2(6, 0)O_2^-$ transition on its right side and is therefore fit by the sum of two Gaussians offset by the known energy interval.

are derived from the errors (one standard deviation) in the line centers as determined by statistics of the fit. This energy difference has been corrected by the scale factor obtained from an O^--S^- experiment,[24] 1.030 ± 0.005, and therefore an additional systematic error of ±3.3 meV should be associated with the value 655.2 meV.

During these measurements the mean ion-beam energy W was 680.00 ± 0.25 eV[24] so that the last term of Eq. (2) contributes 11.57 meV and we take the electron affinity of O to be 1.465 eV. This value was obtained[24] by weighting the possible transitions in photodetachment from O^- by their degeneracies and using the measured value for the electron affinity of O.[5] Hence, with Eq. (9) we obtain the $E^T_{vd}(2, 0) = 821.4$ meV. The energy interval between the $O_2(v' = 2, J = 13)$ and $O_2(v'' = 0, J = 13)$ levels of the $X\,^3\Sigma_g^-$ state is[31] 382.2 meV, so

$$E^T_{vd}(0, 0) = E^T_{vd}(2, 0) - 382.2 \text{ meV} = 439.2 \text{ meV}\,.$$

Since the largest error in the measurement of the vertical detachment energy comes from the uncertainty ±0.005 in our scale correction factor 1.03, it is clear that a procedure which minimizes the energy difference to be measured would improve the over-all accuracy. Hence, we measured the energy difference between the O^- peak and the $a\,O_2(1, 0)O_2^-$ peak. The energy difference corresponding to the transition $a\,^1\Delta g(v' = 1) \rightarrow X\,^2\Sigma_g^-(v'' = 0)$ is known very accurately,[31] so it is possible to

relate the measured vertical detachment energy of the excited state to the electron affinity.

Figure 7 shows the data for this experiment. The measured energy difference was 123.0 ± 1.0 meV. Of the ± 1.0-meV error estimate, ± 0.4 meV is due to the statistics of the fits of the two curves and ± 0.6 meV is due to the error present in the scale correction factor. Reduction of this measured energy difference to $E_{vd}^{T}(0, 0)$ gives a value of 438.8 ± 1.0 meV as compared to our previous value of 439.2 ± 3.9 meV. The excellent agreement obtained demonstrates the consistency of our measured correction factor. We will now consider the value 438.8 ± 1.0 meV as the best value for E_{vd}^{T} $(0, 0)$ and think of the other determination as a confirmation of this value.

Two corrections must still be made to the measured vertical detachment energy in order to obtain the electron affinity. Since the electron affinity refers to the energy difference between the negative ion and the neutral in their rotational ground states, we must make a correction for the rotational energy at both ends of the transition. The beam of negative ions is assumed to possess a Boltzmann distribution of rotational states corresponding to a specific source temperature T. The source temperature can be estimated from observations of the relative populations of the zeroth and first vibrational states of the O_2^- produced. Measurements of the relative intensity of the X $O_2(0, 0)O_2^-$ and X $O_2(0, 1)O_2^-$ transitions, corrected by the proper Franck-Condon factors, determine the relative populations of the two vibrational states. Use of the Boltzmann relation then determines a source temperature of 630 °K. Since individual rotational transitions are not resolved, the data we observe constitute the sum of all of the possible rotational transitions. Further, the final state of the transition is a complex formed by what asymptotically are a p-wave electron and an O_2 molecule in the $a^1\Delta$ state. The total angular momentum left with the O_2 molecule, J', depends upon the initial angular momentum of the negative ion, J'', and the momentum carried away by the outgoing electron. We assume that it is equally probable that the O_2 molecule will be left in a state of higher or lower angular momentum. For example, for a Q branch transition, $J' = J'' - \frac{3}{2}$, $J'' - \frac{1}{2}$, $J'' + \frac{1}{2}$, and $J'' + \frac{3}{2}$ are all possible. We assume that the $J'' + \frac{3}{2}$ and $J'' - \frac{3}{2}$ transitions are equally probable, and that the $J'' + \frac{1}{2}$ transition has the same probability as a $J'' - \frac{1}{2}$ transition. The effect of the outgoing electron is to create a distribution in angular momentum in the possible final states of the molecules, symmetric about the initial angular momentum J''. The P and R branch transitions leave the final complex with one more or one less unit of angular momentum, but the final molecular angular momentum should be distributed symmetrically about J''.

TABLE II. Calculation of rotational-spin-orbit correction factor.

Source temperature (°K)	Spin-orbit splitting (cm^{-1})	Rotational correction (cm^{-1})	Spin-orbit correction (cm^{-1})	Total correction (cm^{-1})	(meV)
630	150	−51.7	62.3	10.6	1.3
530	150	−43.8	62.3	18.5	2.3
730	150	−59.6	62.3	2.7	0.3
630	120	−51.7	74.7	23.0	2.9
630	180	−51.7	49.8	−1.9	−0.2

To calculate the difference in the rotational energies of the upper and lower states, we first calculate an effective J'' which is based upon a Boltzmann population distribution for the rotational levels of the ion for a particular source temperature. For a 630 °K source temperature $J'' = 13.2$. The rotational energy difference, or correction, is then given by

$$-(B_e' - B_e'')J''(J''+1) .$$

The rotational correction for a 630 °K source temperature is -51.7 cm^{-1} or -6.4 meV.

The second correction occurs because the negative-ion state is a $^2\Pi_g$ electronic state and we observe unresolved transitions from both the $^2\Pi_{1/2}$ and $^2\Pi_{3/2}$ states. It is possible to predict[33] that the O_2^- inverted multiplet has a coupling constant of -150 ± 30 cm^{-1}. Assuming that our observed vertical detachment energy comes from transitions from both states with probability proportional to their populations as given by the Boltzmann factor, a second correction must be applied so that the final value of the electron affinity corresponds to the energy difference between the $X\,^3\Sigma_g^-(v' = 0, N' = 0, J' = 1)$ state and the $^2\Pi_{g,3/2}(v'' = 0, J'' = \frac{3}{2})$ state and not from a weighted combination of the $^2\Pi_{1/2}$ and $^2\Pi_{3/2}$ states as the lower state. Using a source temperature of 630 °K we find that the fine-structure splitting of the negative-ion state requires a correction of $+62.3$ cm^{-1} or $+7.7$ meV.

Table II summarizes our calculations of both the rotational and the spin-orbit correction factors. We shall adopt the total correction listed on the first line ($+1.3$ meV) and use the remainder of the table entries to estimate the errors which could be introduced by poor assumptions or incorrect values of the coupling constant or the rotational temperature. When $E_{vd}^{T}(0, 0)$ is corrected for the rotational energy and the ion fine-structure splitting, we obtain 0.440 eV for the electron affinity.

The possible errors in this determination are listed in Table III. They are almost entirely systematic. The total error in the determination of energy differences is ± 0.001 eV. The error introduced by the calculation of the rotational spin-

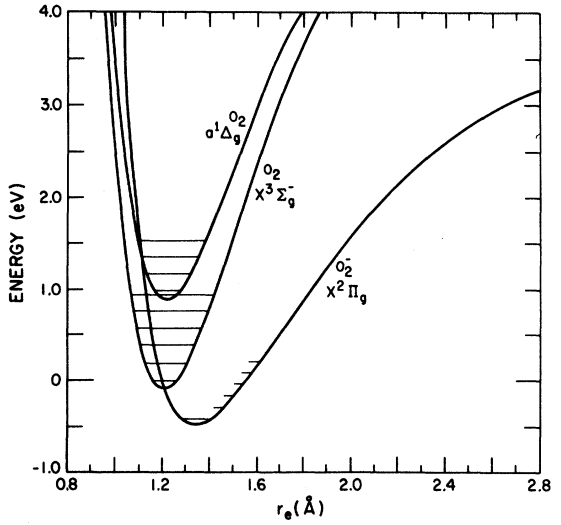

FIG. 8. O_2^- internuclear potential as determined by this experiment. The energy levels shown as solid lines are the levels observed in this experiment.

orbit correction can be estimated from Table II. An error of ±100 °K in the rotational temperature would produce an error of ±0.001 eV. We estimate a maximum error of ±0.002 eV arising from the assumptions made in our calculation of the rotational correction factor. The estimated error of ±30 cm^{-1} in the spin-orbit coupling constant could introduce an error of ±0.0016 eV. An error of ±0.002 eV is introduced from possible mechanical misalignment of the electron detection system.[24] Adding all of the possible errors we arrive at a total error estimate of ±0.008 eV. We feel that this error estimate is conservative and should be considered the maximum sensible error. In any case, the value we obtain for the electron affinity of O_2 is relative to that of O and the latter is taken to be 1.465 eV.[5] Any future change in the O affinity will cause an identical increment in the O_2 affinity.

Since the separated atom limit of O_2^- is $O+O^-$ and we know the electron affinities of O and O_2, as well as the dissociation energy for O_2, it is possible to calculate the dissociation energy for O_2^-. Using 5.116±0.002 eV for the O_2 dissociation energy,[34] we obtain 4.09±0.01 eV for the dissociation energy D_0 of O_2^-.

V. DISCUSSION

The value obtained for the electron affinity is in excellent agreement with the measurements of Pack and Phelps.[10] The results of the two determinations agree within 0.01 eV. It should be remembered that the Pack and Phelps[10] analysis assumed values for the O_2^- spectroscopic constants and did not correct for the O_2^- spin-orbit splitting. When the newly obtained values for ω_e'' and r_e'' are used and a correction for possible O_4^- production is applied the Pack and Phelps data yield[35] an electron affinity of about 0.44 eV. This value would still need to be corrected for the spin-orbit splitting in O_2^- and possibly for the difference between the classical rotational partition function used by Pack and Phelps and its quantum-mechanical analog.

There is also fairly good agreement obtained with the more recent heavy-particle reactive threshold work when Chantry's[22] correction for the thermal motion of the target gas has been made.

The value of r_e'' obtained in this experiment can be compared with that predicted by Badger's[36] rule, 1.374 Å. Since Badger's rule typically does not predict r_e'' better than ±5%,[37] the agreement is considered to be good. Potential curves for O_2^- proposed[28] on the basis of electron-scattering measurements of ω_e'' and the use of Badger's rule to obtain r_e'', agree poorly with our potential in the sense that the $X\ O_2(0,0)O_2^-$ transition would have a vanishingly small Franck-Condon factor while the transition is clearly present in Fig. 2. Figure 8 shows the internuclear potential we have arrived at for O_2^- as well as those for the $X^3\Sigma_g^-$ and $a^1\Delta_g$ states of O_2. The O_2^- potential shown here is a Morse potential and uses the parameters of Sec. IV C near the bottom of the well with a Hulbert-Hirschfelder extension to the dissociation limit.

VI. SUMMARY

The laser photodetachment technique has been used to determine the electron affinity of O_2 as 0.44 eV with a maximum error of ±0.008 eV. The negative-ion internuclear potential has an r_e'' = 1.341±0.010 Å, B_e'' = 1.17±0.02 cm^{-1}, and a dissociation energy D_0 of 4.09±0.01 eV. Angular distribution measurements of the emitted electrons were made and the measured values of the anisotropy parameter β are summarized in Table I.

ACKNOWLEDGMENTS

We are indebted to W. C. Lineberger for his assistance, particularly in our energy scale cali-

TABLE III. Summary of error estimates.

Type	Estimate
Statistical errors	±0.001
Temperature effect on rotational correction	±0.001
Rotational energy calculation	±0.002
Spin-orbit constant	±0.0016
Mechanical misalignment	±0.002
Total	0.0076

bration efforts. We wish to thank D. A. Albritton, A. L. Schmeltekopf, and R. N. Zare for the use of their FCF programs and many helpful discussions. We are grateful to P. J. Chantry for the use of Fig. 1 which is based on a slide he presented at the Gaseous Electronics Conference in October of 1970. Finally, we are indebted to V. Cermak for suggesting the use of N_2O as a source gas.

---

†Research supported by the Advanced Research Projects Agency, The Department of Defense, and was monitored by U. S. Army Research Office–Durham, Box CM, Duke Station, Durham, N. C. 27706, under Contract No. DA-31-124-ARO-D-139.

*Present address: Optical Physics Division, National Bureau of Standards, Washington, D. C.

‡Staff Member, Laboratory Astrophysics Division, National Bureau of Standards.

§Present address: University of Virginia, Department of Aerospace Engineering and Engineering Physics, Charlottesville, Va.

‖Staff Member, Quantum Electronics Division, National Bureau of Standards.

[1]L. B. Loeb, Phys. Rev. 48, 684 (1935).

[2]F. Bloch and N. E. Bradbury, Phys. Rev. 48, 689 (1935).

[3]H. S. W. Massey, *Negative Ions* (Cambridge U. P., London, 1950), p. 28.

[4]R. S. Mulliken, Rev. Mod. Phys. 4, 17 (1932).

[5]L. M. Branscomb, D. S. Burch, S. J. Smith, and S. Geltman, Phys. Rev. 111, 504 (1958).

[6]H. O. Pritchard, Chem. Rev. 52, 529 (1953).

[7]D. S. Burch, S. J. Smith, and L. M. Branscomb, Phys. Rev. 112, 171 (1958); 114, 1652 (1959).

[8]S. Geltman, Phys. Rev. 112, 176 (1958).

[9]R. K. Curran, J. Chem. Phys. 35, 1849 (1961).

[10]J. L. Pack and A. V. Phelps, Phys. Rev. Letters 6, 111 (1961); J. Chem. Phys. 44, 1870 (1966).

[11]R. Fischer, H. Neuert, K. Peuchkert-Kraus, and D. Vogt, Z. Naturforsch. 21a, 501 (1966).

[12]C. L. Pekeris, Phys. Rev. 112, 1649 (1958).

[13]D. B. Dunkin, F. C. Fehsenfeld, and E. E. Ferguson, J. Chem. Phys. 53, 987 (1970).

[14]J. A. D. Stockdale, R. N. Compton, G. S. Hurst, and P. W. Reinhardt, J. Chem. Phys. 50, 2176 (1969).

[15]F. C. Fehsenfeld, D. L. Albritton, J. A. Burt, and H. I. Schiff, Can. J. Phys. 47, 1793 (1969).

[16]D. Vogt, B. Hauffe, and H. Neuert, Z. Physik 232, 439 (1970).

[17]T. L. Baily and P. Mahadevan, J. Chem. Phys. 52, 179 (1970).

[18]K. Lacmann and D. R. Herschbach, Chem. Phys. Letters 6, 106 (1970).

[19]R. J. Celotta, R. Bennett, J. Hall, J. Levine, and M. W. Siegel, Bull. Am. Phys. Soc. 16, 212 (1971).

[20]R. Johnsen, H. L. Brown, and M. A. Biondi, Bull. Am. Phys. Soc. 16, 213 (1971).

[21]S. J. Nalley and R. S. Compton, Chem. Phys. Letters 9, 529 (1971).

[22]P. J. Chantry, J. Chem. Phys. 55, 2746 (1971).

[23]J. Berkowitz, W. A. Chupka, and D. Gutman, J. Chem. Phys. 55, 2733 (1971).

[24]M. W. Siegel, R. J. Celotta, J. Hall, J. Levine, and R. A. Bennett, preceding paper, Phys. Rev. A 6, 607 (1972).

[25]Los Alamos nonlinear least-squares-fitting routine; see, R. H. Moore and R. K. Zeigler, Los Alamos Report No LA 2367, 1960 (unpublished).

[26]J. Cooper and R. N. Zare, J. Chem. Phys. 48, 942 (1968); also in *Lectures in Theoretical Physics* (Gordon and Breach, New York, 1969), Vol. XI-C, p. 317.

[27]W. Holzer, W. R. Murphy, H. J. Berstein, and J. Rolfe, J. Mol. Spectry, 26, 543 (1968).

[28]M. J. Boness and G. J. Schulz, Phys. Rev. A 2, 2182 (1970).

[29]G. Herzberg, *Spectra of Diatomic Molecules*, Vol. I of *Molecular Spectra and Molecular Structure* (Van Nostrand, New York, 1950), pp. 201–202.

[30]L. Herzberg and G. Herzberg, Astrophys. J. 105, 353 (1947).

[31]Reference 29, p. 560.

[32]These programs are from D. L. Albritton, A. L. Schmeltekopf, and R. N. Zare, Diatomic Intensity Factors (Harper and Row, New York, to be published), and have been supplied to us by the authors.

[33]M. Krauss (private communication).

[34]G. Herzberg, Can. J. Phys. 30, 185 (1962).

[35]A. V. Phelps (private communication).

[36]R. M. Badger, J. Chem. Phys. 2, 129 (1934); 3, 710 (1935).

[37]Reference 29, pp. 457–459.